

## HEAT TRANSFER IN A LARGE-PARTICLE FLUIDIZED BED WITH IMMERSSED IN-LINE AND STAGGERED BUNDLES OF HORIZONTAL SMOOTH TUBES

S. S. ZABRODSKY,\* YU. G. EPANOV and D. M. GALERSHTEIN  
 Luikov Heat and Mass Transfer Institute, B.S.S.R. Academy of Sciences,  
 Minsk, B.S.S.R., U.S.S.R.

and

S. C. SAXENA and A. K. KOLAR  
 Department of Energy Engineering, University of Illinois at Chicago,  
 Box 4348, Chicago, IL 60680, U.S.A.

(Received 23 June 1980)

**Abstract**—Experimental results for heat-transfer coefficient between immersed in-line and staggered bundles of horizontal smooth tubes and air-fluidized beds of large particles are reported. The measurements are taken at room temperature and ambient pressure, for spherical millet ( $d_p = 2$  mm) and nonspherical fire clay ( $d_p = 3$  mm) particles. The heat-transfer coefficient values are given as a function of fluidizing velocity (0.6–2.8 m/s), and horizontal and vertical tube pitches. It is found that the heat-transfer coefficient is more sensitive to the changes in the values of the horizontal pitch than those of the vertical pitch. The experimental data for widely spaced tube bundles are described by Zabrodsky's model [14] and his theoretical equation complemented with a modified gas-convective term, equation (6).

The model of Glicksman and Decker [12] concerning the conduction component of heat transfer represents one particular case of Zabrodsky's model i.e. steady-state conduction specific of large and/or fast moving particles, but differs in the account of gas convection, and gives a fair reproduction only of a part of our experimental data for widely spaced tubes. The Staub's model [13] substantially underestimates the experimental results.

### NOMENCLATURE

<p><math>Ar</math>, Archimedes number, <math>d_p^3 g \rho_f (\rho_s - \rho_f) / \mu_f^2</math>;</p> <p><math>b</math>, constant in equation (1);</p> <p><math>C_{pf}</math>, specific heat of gas;</p> <p><math>C_{ps}</math>, specific heat of solid particle;</p> <p><math>D_T</math>, outside diameter of immersed tube;</p> <p><math>d_p</math>, particle diameter;</p> <p><math>g</math>, acceleration due to gravity;</p> <p><math>h_w</math>, heat-transfer coefficient;</p> <p><math>h_{wc}</math>, conductive component of heat-transfer coefficient;</p> <p><math>h_{wcv}</math>, gas convective component of heat-transfer coefficient;</p> <p><math>h_{quiet}</math>, heat-transfer coefficient of quiescent bed;</p> <p><math>h_{wmax}</math>, maximum heat-transfer coefficient;</p> <p><math>k_f</math>, thermal conductivity of fluid;</p> <p><math>k_s</math>, thermal conductivity of a solid particle;</p> <p><math>L</math>, height of fluidized bed;</p> <p><math>L_{mf}</math>, height of bed at minimum fluidization;</p> <p><math>N</math>, fluidization number, <math>U/U_{mf}</math>;</p> <p><math>Nu</math>, Nusselt number, <math>h_w d_p / k_f</math>;</p> <p><math>Nu_f</math>, Nusselt number of gas flow without solid particles, <math>h_w D_T / k_f</math>;</p> <p><math>Nu_T</math>, Nusselt number of gas flow with solid particles, <math>h_w D_T / k_f</math>;</p> <p><math>Pr</math>, Prandtl number, <math>C_{pf} \mu_f / k_f</math>;</p>	<p><math>Re</math>, Reynolds number, <math>U d_p \rho_f / \mu_f</math>;</p> <p><math>Re_{opt}</math>, Reynolds number (optimum), <math>U_{opt} d_p \rho_f / \mu_f</math>;</p> <p><math>S_H</math>, horizontal tube pitch;</p> <p><math>S_V</math>, vertical tube pitch;</p> <p><math>U</math>, superficial gas velocity;</p> <p><math>U_{mf}</math>, minimum fluidizing velocity;</p> <p><math>U_s</math>, average solids velocity;</p> <p><math>U_{opt}</math>, optimum superficial gas velocity.</p> <p><b>Greek symbols</b></p> <p><math>\alpha_f</math>, thermal diffusivity of gas;</p> <p><math>\varepsilon</math>, bubble fraction in the bed;</p> <p><math>\Delta P_d</math>, pressure difference across distributor;</p> <p><math>\varepsilon</math>, average bed voidage;</p> <p><math>\varepsilon_{mf}</math>, bed voidage at minimum fluidization;</p> <p><math>\mu_f</math>, viscosity of gas;</p> <p><math>\nu</math>, kinematic viscosity of gas;</p> <p><math>\rho_f</math>, density of gas;</p> <p><math>\rho_s</math>, density of solid.</p>
---	--

### INTRODUCTION

IN RECENT years, the fluidized-bed combustion of coal has been the subject of intensive research due to its important application in electric power generation. The nearly isothermal nature of the bed, high heat transfer rate between the bed and an immersed surface, as well as an appreciable reduction in environmental pollution are some of the prime factors which make low-temperature fluidized-bed combustion of coal an

\* Deceased.

attractive and viable near-term solution to the problem of energy crisis.

In order to develop efficient fluidized-bed boilers and ensure their reliable design, it is necessary to know the heat transfer characteristics of the tube bundles immersed in the bed. A number of research workers have conducted experiments on bed-to-tube bundle heat transfer and these studies have been reviewed by Saxena *et al.* [1]. Unfortunately, the reported data are mostly restricted to the beds of small particles ( $d_p < 1$  mm), while in practice, the reliable design of steam generators requires the understanding of the behavior of large-particle beds. In such systems, the bubbles move slower than the interstitial gas, whereas in small-particle beds the bubbles move faster than the interstitial gas. For large-particle systems, with the increase in superficial velocity, the slow bubble regime changes to rapidly growing bubbles and finally the turbulent regime sets in. Catipovic *et al.* [2]. In large-particle fluidized beds 'packed' with immersed tube bundles 'classical' gas bubbles with their fairly well-known properties cannot develop. They are distorted due to the closely spaced tubes. Between adjacent tubes of any horizontal row, particle bridging occurs and phase inversion develops, i.e. dense phase of bed becomes discontinuous, while gas voids remain continuous.

Heat transfer between fluidized beds of large particles and surfaces of different configurations has been reported from time to time. Denloye and Botterill [3], and Maskayev and Baskakov [4] have reported data for a vertical tube; Fillippovsky and Baskakov [5] for a vertical plate; Makhorin and Tischenko [6] for a sphere; Traber *et al.* [7] for a coil; and Wright *et al.* [8] for tube bundles. Tamarin *et al.* [9] have examined the performance of immersed staggered horizontal tube bundles and correlated their data by a trigonometric inverse tangent function. Their reported heat transfer coefficient data [9] are considered to be somewhat higher due to the neglect of end losses. Canada and McLaughlin [10] have also investigated large particle systems (600–2600  $\mu\text{m}$ ) with bare and finned horizontal tube banks in the pressure range of one to ten atmospheres. There exist rather a great scatter in their data.

Recently Glicksman and Decker [11], and Staub [12] have attempted to mechanistically model heat transfer to a surface immersed in a fluidized bed of large particles. Glicksman and Decker [11] present the case typical of well-developed fluidized beds of large particles when the temperature decrement of a particle during its contact with the heat transfer surface is negligible. For such a case the unsteady-state heat conduction from the hot surface degenerates to a steady-state one, and the gas convective heat transfer becomes important. Thus, the model of Glicksman and Decker [11] represents essentially a particular case of Zabrodsky's model ([13], pp. 227, 231, 234–235). For such a case, the conductive component of the heat transfer coefficient may be estimated by the

following theoretical equation ([13], equation (10-10); p. 231)

$$h_{wc} = \frac{1.2k_f(1 - \epsilon)^{2.3}}{b + \frac{d_p}{6}} \quad (1)$$

For the gas convective component of the heat-transfer coefficient, Zabrodsky originally proposed ([13], p. 234) to evaluate it in terms of the so-called 'filtrational' part of effective thermal conductivity, which is proportional to  $UC_{pf}\rho_f d_p$ . The convective component therefore increases with increasing superficial fluid velocity, volumetric fluid heat capacity ( $\rho_f C_{pf}$ ), and particle diameter

Several investigators such as Botterill [14] and Baskakov [15], have assumed on the basis of simple two-phase fluidization theory that the gas velocity in the dense phase is always equal to  $U_{mf}$  and therefore the gas-convective component of the heat-transfer coefficient is independent of the Reynolds number. Moreover, it is tacitly assumed that  $h_{wc}$  is independent of  $Re$  for gas velocity between the heater and the first row of particles. It is true that Baskakov [15] did recognize that  $h_{wc} \sim U^{0.3-0.36}$  for gas velocities smaller than  $U_{opt}$  but insist that any dependence of  $h_{wc}$  on  $U$  vanishes beyond the optimum velocity defined by the well-known Todes' equation, see [16]

$$Re_{opt} = Ar/(18 + 5.22\sqrt{Ar}) \quad (2)$$

The experimental data of Canada and McLaughlin [10] do not confirm this and  $h_{wc}$  is not constant at high gas velocities.

Denloye and Botterill [3] also criticise the  $Nu_{conv}$  correlation of Baskakov and Suprun [17] but by using somewhat incorrect point of views. They [3] point out to the large difference between the quiet fluidized bed heat-transfer coefficient and  $h_{wc}$  values calculated by the Baskakov and Suprun [17] equation at low Archimedes numbers. This difference is presumably due to the fact that Baskakov and Suprun equation is more appropriate in describing the 'film nature' of the gas-convective heat-transfer coefficient of a well-developed bubbling fluidized bed than the Denloye and Botterill approach [3]. The latter [3] made an approximation that  $h_{wc}$  equals the total heat-transfer coefficient of a quiet fluidized bed, i.e. without any particle mixing,  $h_{quiet}$ . By doing so they slightly overestimated the heat transfer by gas convection in a quiescent bed neglecting any contribution of steady-state heat conduction. But then by referring  $h_{wc} = h_{quiet}$  to the temperature difference between the probe-surface and the bulk of the bed, i.e. by making no allowance for significant thermal resistance of the quiescent bed itself, they greatly underestimated gas-convective heat transfer for well-developed and vigorously mixing fluidized beds where the above resistance is quite negligible. One may infer that only in the region of high Archimedes numbers, i.e. in the quiescent beds of sufficiently large particles, well-

developed gas convection levels the bed temperature profile and the correspondence between the equations of Denloye and Botterill [3] and Baskakov and Suprun [17] improves.

One additional deficiency of Botterill and Denloye's [3,14] approach is that it neglects *a priori* any possible dependence of  $h_{wcv}$  on superficial gas velocity in any gas flow range without providing evidence. We suggest that further careful experimental work is needed to obtain reliable information concerning the dependence or independence of  $h_{wcv}$  on the gas flow rate in a bubbling bed under different experimental conditions. Tentative empirical formulae (7a) and (9) proposed in the present work are based on the measurements of total  $h_w$  estimates of  $h_{wcv}$  from equation (1), considerations of  $h_{wcv}$  mechanism ([13], pp. 234, 332), and on bed expansion measurements. In equations (7a) and (9) it is assumed that beyond the maximum of  $h_{wcv}$ , it varies as  $U^{0.2}$ . It should be noted that Glicksman and Decker [11] have also assumed the dependence of  $h_{wcv}$  on  $Re$  (i.e.  $U$ ).

Finally, let us consider Staub's model [12] which is directly connected with a specific feature of fluidized bed boilers, i.e. the restriction on the motion of large-particles in the bed with horizontal tube bundles. Staub has developed a correlation for particle Nusselt number in the turbulent flow regime involving particle diameter, densities of gas and solid, and superficial average gas and solids velocities. The last quantity is obtained from the solid circulation model which involves the concept of a mixing length. The latter is taken to be equal to horizontal tube spacing for tube banks.

In view of the above review of the present state of the art, it appears that detailed and systematic investigations of heat transfer characteristics of in-line and staggered tube bundles in fluidized beds of large particles will be very useful. It may be noted that the ability to predict heat-transfer coefficient for large-particle systems with immersed tubes is very limited, and much work remains to be done both in theoretical and experimental areas. The urgency of such efforts is obvious in view of the large number of programs in progress for fluidized bed boilers. Some of our studies made to date in this general direction are reported in the present work.

#### EXPERIMENTAL FACILITY

Heat transfer experiments are conducted in a rectangular (40 cm × 24 cm) fluidized bed column. The column 1.5 m in height is made of steel and is provided with a plexiglas front wall to enable visual observations. The distributor consists of two perforated metal plates with cloth sandwiched between them. 10 mm holes in the distributor plates are located at the vertices of equilateral triangles with 14 mm side. The free area of the perforated plates totals about 10%. The pressure drop across the distributor is measured in the superficial gas velocity range of 0.5–1.13 m/s and correlated by the following relation

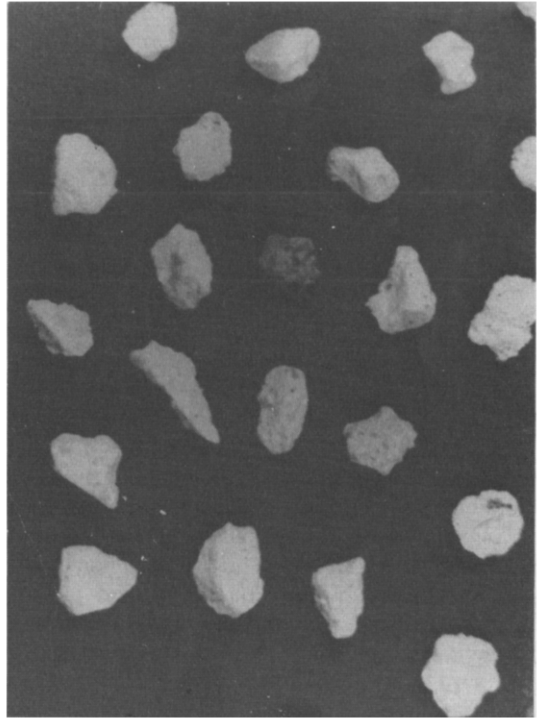


FIG. 1. Microphotograph of fire clay particles.

$$\Delta P_d = 1.6160 U^{1.49}. \quad (3)$$

Here  $\Delta P_d$  and  $U$  are in Pascals and m/s, respectively.

The tube bundles installed in the fluidized bed consist of five to seven rows of horizontal duraluminum tubes 30 mm in the outer diameter. Both in-line and staggered tube arrangements are used, in each case the bottom row being located about 15 cm above the distributor plate. Semicylinders 30 mm in diameter have been fixed to the side walls of the column against the horizontal rows of tubes in order to simulate the extension of the rows of tubes.

The arrangement of the bundles allows any of the tubes to be replaced by the heat-transfer probe. In the staggered tube bundle, the tubes are spaced with equal horizontal,  $S_H$ , and vertical,  $S_V$ , pitches:  $S_H \times S_V = 100 \times 100$ ;  $60 \times 60$  and  $45 \times 45$  mm. The in-line bundles are  $S_H \times S_V = 100 \times 100$ ;  $100 \times 50$ ;  $80 \times 80$ ;  $60 \times 60$  and  $50 \times 50$  mm. Spherical millet seeds are 2.0 mm in diameter ( $\rho_s \approx 1000 \text{ kg/m}^3$ ,  $U_{mf} = 0.55 \text{ m/s}$ ) and nonspherical crushed fire clay, 3 mm in average diameter ( $\rho_s = 2300 \text{ kg/m}^3$ ,  $U_{mf} = 0.95 \text{ m/s}$ ). Figure 1 shows some typical fire clay particles. The static bed height is varied from 270 to 420 mm and the tops of some loose tube bundles project above the bed surface. However, even in these few cases the heat-transfer probe is completely immersed in the bed. The probe is a copper cylinder 30 mm in outer diameter with 5 mm thick walls and with an electric heater inside it, Fig. 2. The probe ends are insulated against excessive heat losses by textolite plugs. Special calib-

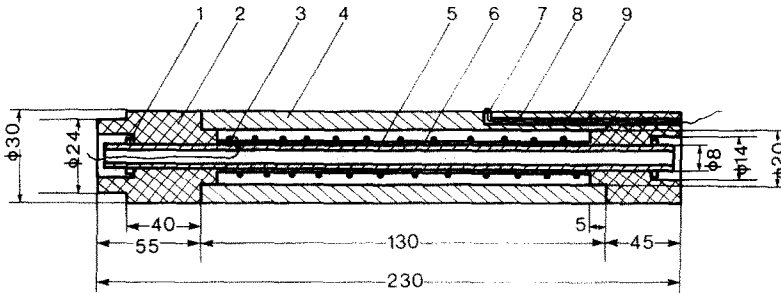


FIG. 2. Schematic of the heat-transfer tube. 1-nut, 2-insulating textolite plug, 3-heating coil, 4-copper tube (wall thickness = 5 mm), 5-stainless steel tube, 6-asbestos board insulation, 7-thermocouple junction, 8-bored hole for thermocouple wires and 9-thermocouple. All dimensions in mm.

ration experiments revealed that the temperature profile in a thick copper wall is uniform up to the largest value of the heat flux. Therefore, it is concluded that wall temperature can be measured by a single and arbitrarily placed thermocouple with its junction being in good contact with the wall. To secure good contact the hot junction is silver soldered to the wall. The thermocouple wires pass through the hole bored along the probe surface as shown in Fig. 2. The ratio of probe length to its diameter is small (4.3) and additional measurements in a wind tunnel (with 0.1% degree of turbulence) have been performed to evaluate the end heat losses. Three tubes have been fixed in the wind tunnel test section having the same orientation to the air flow as in the fluidized bed. The measured heat-transfer coefficients are reproducible within  $\pm 4\%$ . Their comparison with the values calculated from the well-known  $Nu = f(Re, Pr)$  relationship suggests end losses to be about 20%.

The heat-transfer coefficient between the fluidized bed and a tube (probe) in the bundle is measured by the conventional steady-state technique. Bed temperature is measured using a mercury thermometer reading up

to 0.1°C and the power dissipated from the probe-heater by the precision permanent-magnet ammeter and voltmeter. Individual values of the experimental heat-transfer coefficient are correct within  $\pm 5\%$ . The reported overall heat-transfer coefficients are those averaged for three differently placed probes, the individual values for each probe do not differ from the average value by more than 15%. All the three probes are located in the third horizontal row from the bottom. The gas flow rate has been measured with a standard diaphragm accurate to more than  $\pm 3\%$ . All the experiments have been carried out at room temperature and atmospheric pressure.

RESULTS

Figures 3–6 contain the results of experiments for in-line tube bundles with millet and fire clay. The influence of fluidizing velocity,  $U$ , on total heat-transfer coefficient,  $h_w$ , is shown in these figures. In Figs. 5 and 6, in addition, the effect of horizontal and vertical pitches is highlighted. As seen from Fig. 3, in a millet bed experimental  $h_w$  for a given bundle exhibits first a rapid increase with increase in  $U$  but then

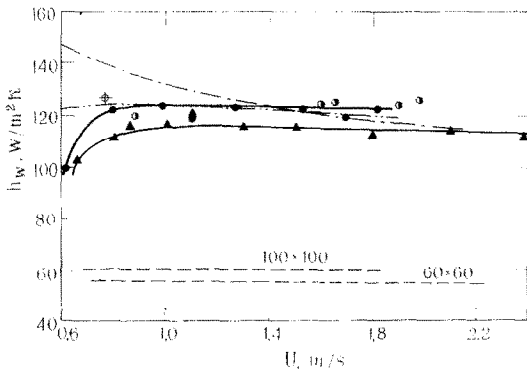


FIG. 3. Variation of  $h_w$  with  $U$  for millet bed and an in-line tube bundle. Experimental: ● (100 × 100), ▲ (60 × 60), ○ (single tube); Calculated: - - - Glicksman and Decker [12], ··· Staub [13], - · - equation (7a); —+— equation (9).

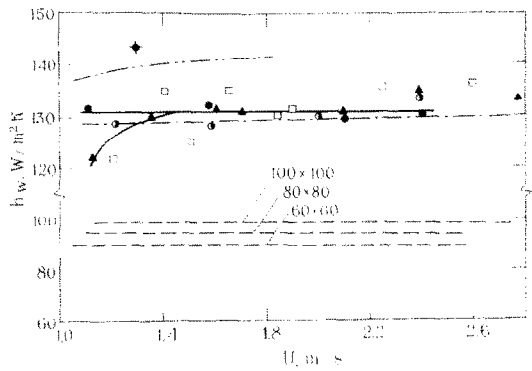


FIG. 4. Variation of  $h_w$  with  $U$  for a fire clay bed and an in-line tube bundle. Experimental: ● (100 × 100), □ (80 × 80), ▲ (60 × 60), ○ (single tube); Calculated: —+— equation (9), the rest of the caption is the same as in Fig. 3.

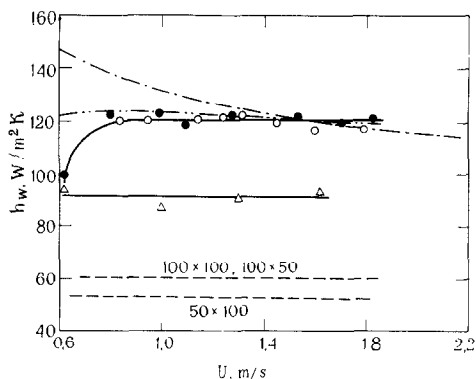


FIG. 5. The effect of  $S_H$  and  $S_V$  on  $h_w$  for a millet bed and an in-line tube bundle. Experimental:  $\circ$  ( $100 \times 50$ ),  $\triangle$  ( $50 \times 100$ ), the rest of the caption is the same as in Fig. 3.

remains constant as  $U$  increases. The maximum of  $h_w$  occurs at a slightly larger value of  $U$  for a closely spaced tube bundle than for a widely spaced bundle. This could be explained by a restrained movement of solid particles in the bundle with closely spaced tubes. It is seen from Fig. 3 that the values of  $h_w$  for a single tube and for a tube bundle with  $S_H = S_V = 100$  mm (hereafter referred to as  $100 \times 100$  bundle) coincide but are consistently greater by a small amount than the values for the tube bundle with  $S_H = S_V = 60$  mm (i.e.  $60 \times 60$  bundle). These results can be readily explained on the basis of possible 'congestion' of the tubes in the latter arrangement where the tubes are located closer to each other in the bundle, and hinder particle motion as is the case with ordinary packing in packed-fluidized beds.

The results for fire clay particles are shown in Fig. 4 for three in-line tube arrangements viz. ( $60 \times 60$ ), ( $80 \times 80$ ) and ( $100 \times 100$ ) bundles and for single tube. The scatter in the data are rather large for ( $80 \times 80$ ) bundle,

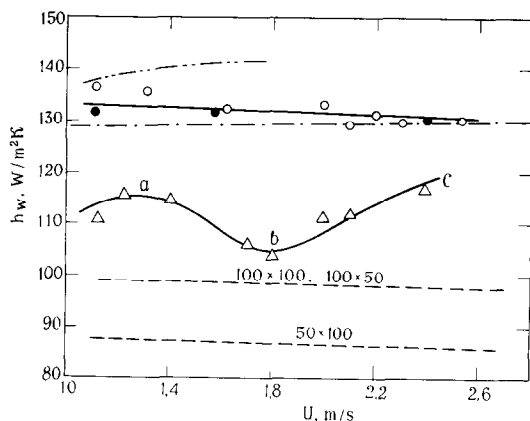


FIG. 6. The effect of  $S_H$  and  $S_V$  on  $h_w$  for a fire clay bed and in-line tube bundle, the rest of the caption is the same as in Figs. 3 and 5.

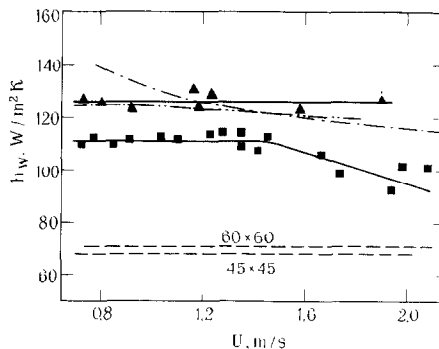


FIG. 7. Variation of  $h_w$  with  $U$  for a millet bed and a staggered tube bundle. Experimental:  $\blacksquare$  ( $45 \times 45$ ), the rest of the caption is the same as in Fig. 3.

but on the basis of all data points it would appear that for  $U > 1.5$  m/s the  $h_w$  values are the same for all of the three bundles. It also appears that for  $U < 1.5$  m/s, the  $h_w$  values for a single tube are in good agreement with ( $100 \times 100$ ) bundle but as expected are larger than for ( $60 \times 60$ ) and ( $80 \times 80$ ) bundles.

The effect of horizontal ( $S_H$ ) and vertical ( $S_V$ ) pitches on  $h_w$  as a function of  $U$  for millet and fire clay are displayed in Figs. 5 and 6, respectively. It is to be noted that the change in  $S_H$  from 100 to 50 mm, with  $S_V$  being constant and equal to 100 mm, significantly reduces  $h_w$ . The influence of the vertical pitch, on the other hand, is negligible as the  $h_w$  values are identical for ( $100 \times 100$ ) and ( $100 \times 50$ ) bundles. This result can be qualitatively explained by the fact that closer arrangement of tubes in a horizontal plane (perpendicular to the direction of the gas flow) hampers solids mixing more appreciably than does the decrease of tube spacing in a vertical plane. This observation is based on experiments where the pitches are varied in a limited range and caution must be exercised in extrapolating this conclusion.

Figures 7 and 8 present the results for staggered tube bundles in millet and fire clay beds respectively and in each case for two tube arrangements, viz. ( $60 \times 60$ ) and ( $45 \times 45$ ) bundles. For the ( $60 \times 60$ ) bundle, the

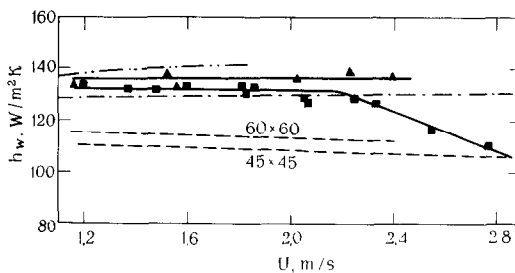


FIG. 8. Variation of  $h_w$  with  $U$  for a fire clay bed and a staggered tube bundle, the rest of the caption is the same as in Fig. 7.

$h_w$  values are larger than those for the (45 × 45) bundle, the difference though appreciable for millet (Fig. 7) is much less pronounced for fire clay (Fig. 8). One notable feature of these results for (45 × 45) bundle is that at  $U/U_{mf} = 2.6$  for millet and 2.3 for fire clay,  $h_w$  decreases sharply with increase in  $U$ . This must be attributed to the decrease in particle concentration near the tube surface and to the increase in the volume of the bed. In fact, during the experiments, it was visually observed that at these high velocities more and more of the bed material got displaced above the (45 × 45) bundle and this would obviously decrease the heat-transfer performance of the bundle. For in-line tube arrays the material displacement evidently needs higher  $U/U_{mf}$  values and appropriate sharp decrease in  $h_w$  is not observed.

An unusual 'wavy' behavior of the  $h_w = f(U)$  curve for the in-line 50 × 100 bundle immersed in the fire clay bed, Fig. 6, may be attributed to particle bridging between adjacent tubes. The smaller is the tube spacing, the lower the  $U/U_{mf}$  value at which bridging appears, especially for the in-line bundles. Below particle bridges there are gas voids, almost free of solids. The 'ab' portion of the wavy curve may be related to the increased number of rather stable bridges formed. Each of them decreases heat-transfer rate because of heat flux reduction under stationary bridge abutments (bases) as well as over the tube surface area in contact with gas voids. The 'bc' portion of the wavy curve corresponds to the increased mobility of bridges, i.e. to more frequent bridge breakdown which results in a gradual heat-transfer rate restoration. No apparent influence of bridging in the same in-line bundle but immersed in the bed of millet may be attributed to the increased bridge instability dealing with a bed-material which is fluidized rather easily in comparison to fire clay. The particle bridging has an insignificant effect on the heat-transfer rate in closely spaced staggered tube bundles due to reduced stability of bridges caused by more developed horizontal components of gas velocity as compared to in-line tube arrays.

#### DISCUSSION

Under the above experimental conditions, with the radiative component being negligible, the total heat-transfer coefficient,  $h_w$ , is assumed to be the sum of the conductive,  $h_{wc}$ , and gas-convective,  $h_{wcv}$ , components

$$h_w = h_{wc} + h_{wcv} \quad (4)$$

In this case when particle size and/or its velocity, and  $C_{ps}\rho_s$  are large enough, the particle temperature remains essentially constant for the residence time of the particle at the heater wall and the unsteady-state heat conduction degenerates to a steady state one. Therefore, we may resort to equation (1). For simplicity, we assume that  $b = 0$  and equation (1) becomes

$$h_{wc} = \frac{7.2k_f(1 - \epsilon)^{2.3}}{d_p} \quad (5)$$

The above relation somewhat overestimates  $h_{wc}$  but this is balanced by the assumption made while deriving equation (1) which approximates the isothermal surfaces in gas between the heat-transfer plate and a spherical particle in contact with it to be flat instead of elliptic. As a result the thickness of the flat gas film with thermal resistance equivalent to that of the gas lens between a particle and the heat transfer surface is  $d_p/15.2$  [18] as compared to  $d_p/6$  assumed in equation (1).

The assumption that  $h_{wcv} \sim U^{0.2} C_{pf}\rho_f d_p$  gives

$$h_{wcv} = BU^{0.2} C_{pf}\rho_f d_p \quad (6)$$

and leads to the following semiempirical equation

$$h_w = \frac{7.2k_f(1 - \epsilon)^{2.3}}{d_p} + BU^{0.2} C_{pf}\rho_f d_p \quad (7)$$

Let us find the numerical value of  $B$  from one experimental point and see whether this value fits all the data presented only for loose tube bundles because equation (7) is not intended to explain the observed dependence of  $h_w$  on the pitch at a particular value of  $U$ . For the in-line 80 × 80 bundle the bed expansion has been measured for both millet and fire-clay particles and average effective bed porosity,  $\epsilon$ , calculated from the following relation reported in [13], p. 288:

$$\epsilon = \epsilon_{mf} + \frac{\Delta P_t}{9\rho_s L_{mf}} \quad (8)$$

where  $\Delta P_t$  is the experimental pressure drop measured across the top part of the fluidized bed above the  $L_{mf}$  level at different  $U$  values. The calculated  $\epsilon$  values are shown in Fig. 9. For both bed materials an essentially unified linear dependence of  $\epsilon$  on  $U$  is observed and there is no 'hysteresis' effect with decreasing and increasing superficial fluidizing velocity.

From Fig. 9, at  $U = 1.7$  m/s the effective bed porosity is  $\epsilon = 0.625$ . The  $h_w$  value is interpolated as 120 W/m<sup>2</sup> K for millet (see Fig. 3), correspond to the measured  $\epsilon$  value for in-line 80 × 80 bundle at  $U =$

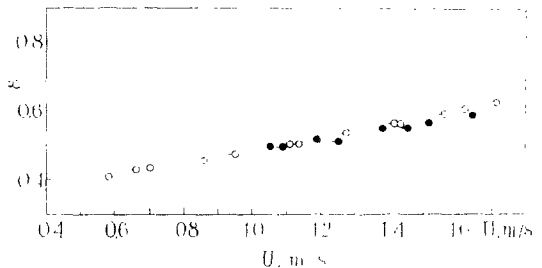


FIG. 9. Variation of  $\epsilon$  with  $U$  for 80 × 80 in-line tube bundle in fire clay and millet beds. Experimental: —●● fire clay; —○○ millet; ●○ measurements at  $U$  increasing; —●○ measurements at  $U$  decreasing.

1.7 m/s. Substitution of these relevant data into equation (7) yields  $B = 26.6 \text{ m}^{-0.2} \text{ s}^{-0.8}$  and this equation takes the form

$$h_w = \frac{7.2k_f(1-\varepsilon)^{2/3}}{d_p} + 26.6U^{0.2}C_{pf}\rho_f d_p \quad (7a)$$

In the absence of information of bed expansion, it is possible to make an approximate estimate of  $h_{w \max}$  which is of special interest when dealing with fluidized beds and because of the relatively flat nature of the  $h_w$  vs  $U$  characteristic. Assuming that at  $U = U_{\text{opt}}$  where the heat-transfer coefficient is maximum  $\varepsilon_{\text{opt}} \approx \varepsilon_{mf}$ , one readily obtains for large-particle beds from equation (7a)

$$h_{w \max} \approx \frac{7.2k_f(1-\varepsilon_{mf})^{2/3}}{d_p} + 26.6U_{\text{opt}}^{0.2}C_{pf}\rho_f d_p \quad (9)$$

where  $U_{\text{opt}}$  may be determined from the well-known Todes' equation [18]

$$Re_{\text{opt}} \equiv \frac{U_{\text{opt}}d_p}{\nu} = \frac{Ar}{18 + 5.22\sqrt{Ar}} \quad (10)$$

The  $h_w$  values calculated from equations (7a) and (9) as applied to the relevant experimental conditions are shown in Figs. 3–8. The numerical value of  $B$  calculated from a single bed-expansion and heat transfer measurement succeeds rather well in reproducing  $h_w$  values obtained under different conditions for widely spaced tube bundles immersed in millet and fire-clay fluidized beds.

In addition, in Figs. 3–8 the  $h_w$  values are also plotted as obtained from Glicksman and Decker's equation [11], and from Staub's correlation [12]. Glicksman and Decker [11] have suggested for a horizontal tube

$$Nu = (1 - \delta) [9.42 + 0.042RePr] \quad (11)$$

Here the bubble fraction of the bed is not experimentally determined but is estimated from the following relation [19]

$$\delta = 1 - \frac{1 - \varepsilon}{1 - \varepsilon_{mf}} \quad (12)$$

$\varepsilon$  is calculated from the following equation given by Staub and Canada [20]

$$U/\varepsilon = 1.05U + \frac{1 - \varepsilon_{mf}}{\varepsilon_{mf}} U_{mf} \quad (13)$$

and  $\varepsilon_{mf}$ , from the following Ergun correlation [19] as modified by Geldart and Cranfield [21]

$$1.75\rho_f U_{mf}^2 + 180 \frac{1 - \varepsilon_{mf}}{d_p} \times \mu_f U_{mf} - \varepsilon_{mf}^3 d_p (\rho_s - \rho_f) g = 0 \quad (14)$$

Equation (11) leads to the results which are in good agreement with experimental data for fire clay, Figs. 4, 6 and 8. The agreement is poorer for the beds of millet, Figs. 3, 5 and 7, where the calculated  $h_w$  values decrease too rapidly with increase of  $U$  in contradiction with the experimental results.

Staub [12] has developed a model of solids circulation for a turbulent flow regime and then used it to obtain a heat transfer model for the beds of large particles with immersed tube bundles.

The solids circulation model gives

$$U_s = 0.42(1 - \varepsilon)S_H^{0.4} \quad (15)$$

and the heat transfer coefficient is evaluated from the following normalized relation

$$\frac{Nu_t}{Nu_f} = \left[ 1 + \left( \frac{150}{d_p} \right)^{0.73} \left( \frac{\rho_s U_s}{\rho_f U} \right)^{0.45} \right] \quad (16)$$

Here  $d_p$  is in  $\mu\text{m}$ . The Nusselt number for the gas flow across the tube bundle in the absence of solid particles,  $Nu_f$ , is obtained from Colburn's correlation, McAdams [22].

The  $h_w$  values calculated from equation (16) are plotted in Figs. 3–8. It is observed that this model predicts  $h_w$  values which are consistently smaller than the experimental data. The difference in the two sets of values is also substantial. The calculated  $h_w$  values are almost constant over the entire range of  $U$ .

According to Staub [12] the value of  $Nu_f$  is obtained from one of the correlations for tube bundles [22], with  $U$  as the reference velocity. This successfully predicts the observed trend of increasing  $h_w$  with increase in  $S_H$ . However, in the development of tube bundle correlations [22], the reference velocity employed is the gas velocity which is obtained by taking into consideration the reduced flow area due to tube insertion in the bed and not the superficial gas velocity,  $U$ . This reference velocity is obviously more than  $U$ , and  $h_w$  based on this reference velocity is found to decrease with increasing  $S_H$ . It must be noted that this trend is opposite to the observed one and therefore selection of the reference velocity is important, and the one proposed by Staub [12] is different from that used in the development of original correlations for  $Nu_f$  [22].

## CONCLUSIONS

The interpretation of the experimental results for heat transfer data in fluidized beds of large particles and tube bundles, and their comparison with existing correlations lead to the following general conclusions:

1. The horizontal pitch significantly affects the heat transfer from a tube bundle. The influence of the vertical pitch is relatively insignificant.
2. The simplified theoretical equation (5) for the conductive heat transfer complemented with the semiempirical gas-convective term, equation (6) fits fairly well the experimental data for widely spaced tube bundles.
3. The Glicksman and Decker correlation also fits well the experimental data for widely spaced tube bundles immersed in the fluidized beds of fire clay but agreement between equation (11) and experimental results with the beds of millet is poorer.

4. The heat transfer measurements in a wide range of Reynolds numbers for large particles are needed to improve the  $h_{wec}$  estimates. There is no sufficient reason to identify  $h_{wec}$  with the total heat transfer coefficient of a quiescent fluidized bed without due correction for the thermal resistance of the quiescent bed.

*Acknowledgements*—This work is partly supported by the United States National Science Foundation under grant No. ENG 77-08780 A01 in a collaborative research program between U.S.A. and U.S.S.R. The authors are also grateful to Dr. S. N. Upadhyay for his assistance in checking some of the calculations presented in this paper.

#### REFERENCES

1. S. C. Saxena, N. S. Grewal, J. D. Gabor, S. S. Zabrodsky and D. M. Galershtein, Heat transfer between a gas fluidized bed and immersed tubes. *Adv. Heat Transfer* **14**, 149 (1978).
2. N. M. Catipovich, G. N. Jovanovic and T. J. Fitzgerald, Regimes of fluidization for large particles, *A.I.Ch.E. J* **24**(3), 543 (1978).
3. A. O. O. Denloye and J. S. M. Botterill, Bed to surface heat transfer in a fluidized bed of large particles, *Powder Technol.* **19**, 197 (1978).
4. V. K. Maskaev and A. P. Baskakov, Characteristics of external heat transfer in fluidization bed of coarse particles, *J. Engng Phys.* **24**(4), 411 (1973).
5. N. F. Filippovskii and A. P. Baskakov, Study of the temperature field near a hot plate in a fluidized bed and of the heat transfer between them, *J. Engng Phys.* **22**(2), 159 (1972).
6. K. Makhorin and A. T. Tishchenko, *High Temperature Fluidized Bed Units*. Tekhnika Press, Kiev (1966).
7. D. G. Traber, V. B. Sarkits and I. P. Mukhlenov, Heat transfer from a suspended bed of granular materials to the heat transfer surface, *Zh. Prikl. Khim.* **33**, 10 (1960).
8. S. J. Wright, H. C. Ketley and R. G. Hickman, The combustion of coal in fluidized beds for firing shell boilers, *J. Inst. Fuel.* **42**(341), 235 (1969).
9. A. I. Tamarin, S. S. Zabrodsky and Y. G. Yepanov, Heat transfer between a horizontal staggered tube bundle and a fluidized bed, *Heat Transfer—Soviet Res.* **8**(5), 51 (1976).
10. G. S. Canada and M. H. McLaughlin, Large particle fluidization and heat transfer at high pressures, *A.I.Ch.E. Symp. Ser.* **74**(176), 27 (1978).
11. L. R. Glicksman and N. Decker, Heat transfer in fluidized beds with large particles, Private Communication.
12. F. W. Staub, Solids circulation in turbulent fluidized beds and heat transfer to immersed tube banks, *J. Heat Transfer* **101**, 391 (1979).
13. S. S. Zabrodsky, *Hydrodynamics and Heat Transfer in Fluidized Beds*. MIT Press, Cambridge (1966).
14. J. S. M. Botterill, *Fluid-Bed Heat Transfer*. Academic Press, London (1975).
15. A. P. Baskakov, *Heat and Mass Transfer Processes in a Bubbling Fluidized Bed*, p. 142. Metallurgiya, Moscow (1978).
16. M. E. Aerov and O. M. Todes, *Hydraulic and Thermal Fundamentals of the Operation of Steady-State and Fluidized Bed Granular Bed Apparatuses*, p. 474. L. Khimiya (1968).
17. A. P. Baskakov and N. M. Suprun, Determination of the convective component of the heat-transfer coefficient to a gas in fluidized bed, *Int. Chem. Engng* **12**, 324 (1972).
18. V. D. Dunsy, S. S. Zabrodsky and A. I. Tamarin, On the mechanism of heat transfer between a surface and a bed of moving particles, *Proc. 3rd Int. Heat Transfer Conf.*, Chicago, Vol. 4, Paper 144 (1966).
19. D. Kunii and O. Levenspiel, *Fluidization Engineering*. R. E. Krieger, Huntington, NY (1977).
20. F. W. Staub and G. S. Canada, Effect of tube bank and gas density on flow behavior and heat transfer in fluidized beds, in *Fluidization*. Cambridge University Press, Cambridge (1978).
21. D. Geldart and R. R. Cranfield, The gas fluidization of large particles, *Chem. Engng J.* **3**, 211 (1972).
22. W. H. McAdams, *Heat Transmission*, 3rd edn. McGraw Hill, New York.

#### TRANSFERT THERMIQUE DANS UN LIT FLUIDISE A GROSSES PARTICULES AVEC UN FAISCEAU IMMERGE DE TUBES EN LIGNE ET HORIZONTALS

**Résumé**— On présente des résultats expérimentaux sur le coefficient de transfert thermique entre un faisceau de tubes lisses, horizontaux, en ligne et des grosses particules dans un lit fluidisé à l'air. Les mesures sont faites à la température et à la pression ambiante pour des particules sphériques de millet ( $d_p = 2$  mm) et non-sphériques de réfractaire ( $d_p = 3$  mm). Les valeurs du coefficient de transfert sont données en fonction de la vitesse de fluidisation (0,6 à 2,8 m/s), et des pas verticaux et horizontaux entre tubes. On montre que le coefficient de transfert thermique est plus sensible au changement de pas horizontal qu'au changement de pas vertical. Les résultats expérimentaux pour des tubes très espacés sont donnés par le modèle de Zabrodsky [14] et son équation théorique (6) est complétée par un terme modifié de convection gazeuse.

Le modèle de Glicksman et Decker [12] concernant la composante de conduction dans le transfert thermique représente un cas particulier du modèle de Zabrodsky, celui de la conduction permanente des particules grosses et/ou à déplacement rapide, mais il diffère dans la prise en compte de la convection gazeuse et il reproduit convenablement seulement une partie de nos résultats pour les grands espaces entre tubes. Le modèle de Staub [13] sous-estime nettement les résultats expérimentaux.



### WÄRMEÜBERTRAGUNG IN EINEM GROBKÖRNI- GEN WIRBELBETT MIT IN REIHE UND VERSETZT ANGEORDNETEN HORIZONTAL- EN GLATTRÖHRBÜNDELN

**Zusammenfassung** — Es werden Versuchsergebnisse für den Wärmeübergangskoeffizienten zwischen in Reihe und versetzt angeordneten horizontalen Glattrohrbündeln und grobkörnigen Luftwirbelschichten angegeben. Die Messungen werden für sphärische Hirsekörner ( $d_p = 2$  mm) und nichtsphärische Tonerdepartikel ( $d_p = 3$  mm) bei Raumtemperatur und Umgebungsdruck durchgeführt. Die Werte für den Wärmeübergangskoeffizienten werden als Funktion der Fluidisierungsgeschwindigkeit (0,6 bis 2,8 m/s) und der horizontalen und vertikalen Rohrabstände angegeben. Es ergibt sich, daß der Wärmeübergangskoeffizient stärker von den Änderungen der Werte des horizontalen Abstands als von jenen des vertikalen Abstands beeinflusst wird. Die experimentellen Daten für Rohrbündel mit großer Teilung werden durch das Modell von Zabrodsky [14] beschrieben, und seine theoretische Gleichung wird mit einem modifizierten Gaskonvektionsterm, Gl. (6), vervollständigt.

Das Modell von Glicksman und Decker [12], das die Wärmeleitungs-komponente der Wärmeübertragung betrifft, stellt einen Sonderfall des Zabrodsky'schen Modells dar, und zwar stationäre, hauptsächlich bei großen und/oder sich schnell bewegenden Partikeln auftretende Wärmeleitung, unterscheidet sich aber in der Berücksichtigung der Gaskonvektion und gibt nur einen Teil unserer experimentellen Daten für Rohre mit großer Teilung gut wieder. Das Modell von Staub [13] liefert gegenüber den experimentellen Ergebnissen wesentlich zu niedrige Werte.

### ТЕПЛООБМЕН МЕЖДУ ПСЕВДООЖИЖЕННЫМ СЛОЕМ КРУПНЫХ ЧАСТИЦ И ПОГРУЖЕННЫМИ В НЕГО КОРИДОРНЫМИ И ШАХМАТНЫМИ ПУЧКАМИ ГОРИЗОНТАЛЬНЫХ ГЛАДКИХ ТРУБ

**Аннотация** — Приведены экспериментальные данные по коэффициенту теплообмена между псевдоожигенным воздухом слоем крупных частиц и погруженными в него коридорными и шахматными пучками гладких труб. Измерения проведены при комнатной температуре и атмосферном давлении. Дисперсным материалом служило просо ( $d_p = 2$  мм) и дробленый шамот ( $d_p = 3$  мм). Коэффициент теплообмена представлен в виде функции от скорости ожигения (0,6 до 2,8 м/с) и горизонтального и вертикального шагов между трубами. Было установлено, что коэффициент теплообмена более чувствителен к изменению величины горизонтального шага, чем вертикального. Экспериментальные данные для нетесных пучков труб описываются моделью Забродского [14], в теоретическое уравнение которой введен модифицированный конвективный член [уравнение (6)].

Модель Гликсмана и Декера [12], что касается кондуктивной составляющей теплообмена, представляет собой частный случай модели Забродского, а именно, рассматривает стационарный кондуктивный перенос, который характерен для крупных и/или быстро движущихся частиц, но отличается в учете конвективной составляющей и дает хорошее совпадение только с частью наших экспериментальных данных для нетесных пучков труб. Модель Стауба [13] дает значительное занижение по сравнению с экспериментом.